Life Sciences Student Journal
2025, Vol3, No2 pp 54-70
DOI:10.22034/LSSJ.2025.133

Evaluation of PI3K/AKT, EGFR, P53, Wee1 genes expression in cervical cancer cells induced by chitosan-cisplatin nanoparticles Enhanced with Gemcitabine

Yasamin Kharatian[1], Elham Rajab Beigi[1], Alma Davarnia[1], Mohammad Reza Nourani[2*]

1.Department of Cellular and Molecular Biology, Faculty of Advanced Sciences and Technology, Tehran Medical Sciences, Islamic Azad University, Tehran, Iran

2.Tissue Engineering and Regenerative Medicine Research Center, Baqiyatallah University of Medical Sciences, Tehran, Iran

* Corresponding author: Mohammad Reza Nourani , Email: r.nourani@yahoo.com

Yasamin Kharatian
Genetics MSc

Article Type:
Research article

Article Info:
Received: 21 Nov . 2024
Revised: 30 Dec. 2024
Accepted: 3 February 2025
ePublished: 4 March 2025

Key words: PI3K/AKT, EGFR, P53, Wee1 genes, cervical cancer, chitosan-cisplatin nanoparticles, gemcitabine

Abstract

Introduction: Cervical cancer remains one of the leading cancers in the world and is considered one of the worst health issues affecting most developing countries. Infection by human papillomavirus induces critical cellular pathways such as PI3K/AKT, EGFR, P53, and Wee1. In the present study, the researchers investigate the effects that chitosan-cisplatin nanoparticles combined with gemcitabine will have on cervical cancer cells in the name of altering the expression of some important genes.

Materials and Methods: The current study deals with the preparation, cisplatin and gemcitabine loading on chitosan nanoparticles, cultural manipulations of a HeLa cell line and its treatment using different concentration series of nanoparticles, characterization using UV-Vis Spectroscopy, FTIR and SEM, followed by cytotoxic effects analyzed in the MTT assay and estimation of gene expressions of PI3K, AKT, EGFR, P53 and Wee1 by real time polymerase chain reaction.

Results: The prepared chitosan nanoparticles had particle sizes that ranged between 18.61 nm to 211.4 nm; besides, there was effective drug loading. The MTT assay displayed that CSNps-CP-Gem caused significant inhibition of viability, with the IC50 values calculated as 6.005 µg/mL and 4.050 µg/mL at 24 and 48 hours, respectively. Gene expression analysis showed a significant down-regulation of PI3K, AKT, and EGFR to 0.737, 0.664, and 0.578, respectively, while the P53 was upregulated two-fold to 2.274. Wee1 expression was down-regulated but not at a statistically significant level.

Discussion: These results have shown that chitosan-cisplatin nanoparticles, combined with gemcitabine, may effectively enhance the cytotoxicity to cervical cancer cells with very minimal toxicity to normal tissues. Modulation of some key signaling pathways indicates a possible mechanism for the observed therapeutic effects. The present study hence underlines the potential of nanoparticle-based drug delivery systems for the improvement of treatment outcomes in cervical cancer and thus warrants further investigation into their clinical applications.

1. Introduction

Cervical cancer is the second most common cancer in the world. It is the fourth leading cause of cancer-related deaths among women globally, with over 85% of incidents and deaths occurring in developing countries (1). Most cervical cancer cells infected with human papillomavirus are known known to express viral oncogenes

E6 and E7, which suppress cellular regulatory proteins that play crucial roles in growth, differentiation, survival, apoptosis, and genome stability.

Regions with the highest incidence of cervical cancer include the Caribbean, Central American countries, South America, Sub-Saharan Africa, and South Asian countries. Even in developed countries like the United States (US), cervical cancer remains a persistent threat. In 2016, approximately 12,990 cases of cervical cancer and related deaths were reported in the United States, with an average age of diagnosis around 47 years (2, 3)

The cervix is a complex structure that includes a mucus-secreting columnar epithelium in the endocervical canal and a stratified squamous epithelium covering the exocervix. The squamocolumnar junction of these epithelia is a critical area in the cervix that is highly susceptible to viral neoplastic changes. Cervical carcinoma encompasses various histological subtypes, including squamous cell adenocarcinoma, neuroendocrine, papillary serous, and clear cell types (4). Most cases of cervical cancer are primarily caused by infection with human papillomavirus (HPV). To combat cervical cancer, prevention, early detection, and classification are of great importance. Prevention includes measures such as widespread HPV vaccination, which helps reduce the risk of developing cervical cancer (5). Early detection is essential for identifying the disease in its initial stages when it is more treatable and associated with better outcomes. This typically involves regular screenings such as Pap smears or HPV tests to identify any abnormalities in cervical cells (6).

In cervical cancer, signaling pathways such as PI3K/AKT and EGFR play a key role in regulating the growth and survival of cancer cells, with mutations or disruptions in these pathways potentially leading to cancer cell proliferation and invasion. Additionally, the genes P53 and WEE1 serve as important regulators of the cell cycle and apoptosis, making them significant targets for cancer inhibition.

P53: Cervical cancer is caused by infection with high-risk HPV, leading to the immortalization of cervical cells and the development of cervical intraepithelial neoplasia (CIN). Dysplasia can progress to invasive cervical cancer. HPV is a DNA virus that contains eight open reading frames, with the oncogenic proteins E6 and E7 playing roles in carcinogenesis. E7 enhances E2F activity by phosphorylating pRB, which promotes cell cycle progression and stimulates apoptosis. E6 reduces apoptosis by increasing the degradation of p53 through E6AP and suppressing the p53 pathway (7). Additionally, E6 inhibits the expression of Notch1 by inactivating p53 and also affects the expression of ErbB2. Both E6 and E7 can independently and synergistically immortalize cervical cells, and in vitro studies have confirmed the simultaneous function of these two proteins in carcinogenesis (8).

PI3Ks are categorized into three classes: Class I, II, and III, each with unique subunits and functions, except for the common Akt subunit. Class I PI3Ks, which include p110 and p85, activate downstream kinases and are further divided into four isoforms: p110α, p110β, p110γ, and p110δ, with PIK3CA being notable for mutations in cancers(9). Class II PI3Ks, lacking regulatory subunits, consist of isoforms C2α, C2β, and C2γ, with C2α playing a significant role in breast cancer(53). Class III PI3K, or VPS34, is essential for autophagy and macrophage phagocytosis (54) . Activation of the PI3K/Akt pathway is crucial for cancer progression and is influenced by factors like RTK family members and B cell antigen receptors (10).

EGFR signaling plays a crucial role in regulating several metabolic processes essential for the proliferation of cancer cells, including fatty acid and pyrimidine biosynthesis as well as glucose catabolism (11). It promotes these metabolic pathways either directly by phosphorylating rate-limiting enzymes or indirectly through the activation of the MYC transcription factor and the AKT signaling cascade. In glioblastoma multiforme, oncogenic EGFR signaling via EGFRvIII stimulates PI3K/AKT-dependent nuclear translocation of the regulatory protein SREBP-1 and the expression of low-density lipoprotein receptor (LDLR) (12). The increase in LDLR facilitates cholesterol uptake by bypassing negative feedback regulation, highlighting a metabolic vulnerability, as these cells rely on cholesterol absorption and are particularly sensitive to inhibitors of fatty acid and cholesterol biosynthesis (94). density lipoprotein receptor (LDLR). The increase in LDLR facilitates cholesterol uptake by bypassing negative feedback regulation, highlighting a metabolic vulnerability, as these a meta-

vulnerability, as these cells rely on cholesterol absorption and are particularly sensitive to inhibitors of fatty acid and cholesterol biosynthesis (13).

The WEE1 gene, located on chromosome 11, encodes a protein kinase that plays a crucial role in regulating the cell cycle, particularly at the G2/M checkpoint (14). By phosphorylating and inhibiting cyclin-dependent kinases (CDKs), WEE1 prevents premature entry into mitosis, allowing for DNA repair. Dysregulation of WEE1 can lead to uncontrolled cell proliferation and contribute to tumorigenesis, making it an attractive target for cancer therapies. In cervical cancer, WEE1 may be upregulated due to DNA damage from high-risk HPV infections, enabling cancer cells to survive despite genomic instability. Targeting WEE1 with inhibitors could potentially sensitize cervical tumors to DNA-damaging agents, presenting a promising strategy for treatment (15).

Gemcitabine is a chemotherapy drug used as a nucleoside analog for treating various types of cancer. It was first approved by the FDA in 1996 for pancreatic cancer and has since been utilized for other cancers, including lung, bladder, and ovarian cancer (16). The drug works by entering cancer cells and becoming activated, substituting for cytidine triphosphate (CTP) in the DNA chain. This incorporation halts DNA replication and consequently stops cell division, leading to cancer cell death. Gemcitabine is typically administered via intravenous injection and is often combined with other chemotherapy agents like cisplatin to enhance its effectiveness. Known for its broad anticancer activity and relatively low side effects, it is recognized as an effective chemotherapy option. However, gemcitabine can cause side effects such as bone marrow suppression (leading to reduced blood cell counts), nausea, vomiting, and fatigue, necessitating careful medical monitoring during treatment (17). Clinical studies have extensively evaluated gemcitabine, and it has been accepted as part of standard treatment protocols for several cancer types. Additionally, combining this drug with other anticancer agents has shown significant improvements in treatment outcomes in some cases (18).

Cisplatin is a crucial chemotherapy drug widely used in the treatment of various cancers, including testicular, ovarian, bladder, and non-small cell lung cancer (19). Its primary mechanism involves forming covalent bonds with DNA, leading to cross-linking that prevents DNA replication and transcription, ultimately inducing apoptosis in cancer cells. Often employed in combination with other agents, cisplatin enhances treatment efficacy and can overcome resistance. However, its use is accompanied by significant side effects such as nephrotoxicity, nausea, and bone marrow suppression. Ongoing research aims to develop formulations that minimize toxicity and explore combinations with phytochemicals to improve outcomes and reduce side effects. Despite challenges, cisplatin's effectiveness makes it a cornerstone in cancer chemotherapy (20).

To reduce the side effects of chemotherapy drugs and minimize their use, as new therapeutic methods, medications are loaded into chitosan nanoparticles as a career for slow release, thereby enhancing their therapeutic effects. Chitosan nanoparticles have gained attention as an effective drug carrier in targeted cancer therapies due to their unique properties, including high biocompatibility, the ability to load various drugs, and controlled release (21). The use of pharmaceutical compounds such as cisplatin and gemcitabine, which are potent chemotherapy agents for treating various cancers, in combination with chitosan nanoparticles can enhance therapeutic efficacy (22).

The aim of this project is to evaluate the expression of key genes involved in the PI3K/AKT, EGFR, P53, and WEE1 signaling pathways in cervical cancer cells treated with chitosan-cisplatin nanoparticles combined with gemcitabine. By investigating the molecular effects of this novel therapeutic approach, the project seeks to elucidate the potential of chitosan nanoparticles to enhance the efficacy of chemotherapy while minimizing side effects and Dosage. This study aims to provide insights into the underlying mechanisms of action, contributing to the development of more effective and targeted treatment strategies for cervical cancer. combined with gemcitabine. By investigating the molecular effects of this novel therapeutic approach, the project seeks to elucidate the potential of chitosan nanoparticles to enhance the efficacy of chemotherapy while minimizing side effects and Dosage. This study aims to provide insights into the underlying mechanisms of action, contributing to the development of more effective and targeted

treatment strategies for cervical cancer.

2 Materials and Methods

2.1 Preparation of chitosan nanoparticle

According to the study by Nair et al. [80], a 1% acetic acid solution was first prepared in deionized water. Chitosan was dissolved in the acetic acid solution to obtain a chitosan solution of 0.5 mg/mL (15 mg of chitosan in 30 mL of 1% acetic acid). The chitosan solution was stirred overnight at room temperature using a magnetic stirrer. The resulting solution had a pH of approximately 3.6, which was adjusted to 4.7-4.8 using a 20% w/w sodium hydroxide solution. The chitosan solution was then filtered through a syringe filter (0.45-micron pore size, Millipore, USA) to remove any undissolved particles. Separately, a 0.5 mg/mL solution of tripolyphosphate (TPP) was prepared in ultra-pure water and also filtered using a syringe filter (0.45-micron pore size, Millipore, USA).

2.2 Addition of Drug-Loaded Chitosan Nanoparticles (Gem + CP)

Cisplatin Cisplatin (CP) powder (شرکت)and gemcitabine were mixed with deionized water to create a solution with a concentration of 50 mg/mL. Dropwise additions of the prepared CP and gemcitabine solutions were introduced into the chitosan solution (CS) at a drug-to-carrier ratio of 1:1. The mixture was then thoroughly blended using a sonicator with a probe sonication method. After mixing, the supernatant was discarded, and the precipitate was freeze-dried. The resulting nanoparticles were stored at 4 degrees Celsius for use in subsequent studies.

2.3 Confirmation Tests for Nanoparticle Synthesis

The formation of the biosynthesized chitosan nanoparticles was examined using a UV-VIS spectrophotometer within the wavelength range of 200-800 nm. The size and shape of the biosynthesized chitosan nanoparticles were determined using Field Emission Scanning Electron Microscopy (FE-SEM). Additionally, Energy Dispersive X-ray Spectroscopy (EDX) and Fourier Transform Infrared Spectroscopy (FT-IR) were employed to confirm the characteristics of the biosynthesized chitosan nanoparticles.

2.4 UV-VIS Spectroscopy

To investigate the formation of chitosan nanoparticles, UV-VIS spectra were recorded using a spectroscopic device. After ultrasonic treatment and centrifugation of the synthesized chitosan nanoparticles, 100 µL of the sample was placed into a microtube and analyzed with a spectrophotometer in the wavelength range of 200 to 800 nm.

2.5 FT-IR Spectroscopy

Fourier Transform Infrared Spectroscopy (FT-IR) is based on the absorption of radiation and the examination of molecular and polyatomic ion vibrations. This technique serves as an advanced and powerful method for determining the structure and measuring chemical species. It is particularly useful for identifying organic compounds, as the spectra obtained from these compounds are often complex and contain multiple maxima and minima that can be used for comparison and identification.

In this study, FT-IR was utilized to identify and determine the types of functional groups and bonds present in the synthesized chitosan nanoparticles. For this purpose, 4 µL of each synthesized chitosan nanoparticle sample was analyzed in liquid form within the spectral range of 4000-400 cm^{-1} using a Brucker device.

2.6 Characterization of Synthesized Chitosan Nanoparticles Using FE-SEM

To investigate the size and shape of the synthesized chitosan nanoparticles, Field Emission Scanning Electron Microscopy (FE-SEM) was employed. Since the samples need to be prepared in a dry state for imaging, the resulting precipitate was dried in an incubator at 37 degrees Celsius for 48 hours, after which it was converted into a powder.

for imaging, the resulting precipitate was dried in an incubator at 37 degrees Celsius for 48 hours, after which it was converted into a powder.

To prevent the formation of static charge during imaging, which could lead to image instability, the samples were required to have electrical conductivity. Therefore, the samples were fixed onto the microscope stubs and coated with a layer of gold using a sputter coater. This gold layer provided the necessary electrical conductivity and allowed for the dissipation of surface electrons, resulting in im-

2.7 Cell Culture

In this study, the HeLa cell line was obtained from the Genetic Resource Center (IBRC C11311) and cultured according to standard protocols. The cells were grown in DMEM medium supplemented with 10% FBS and 1% penicillin-streptomycin under conditions of 37°C and 5% CO2. The morphology, viability, and cell count were regularly monitored using an inverted microscope. After the cells reached a minimum of 70% confluency, they were passaged, and if necessary, the cells were frozen for later stages.

2.8 Determination of Cell Viability Percentage

The MTT assay was used to evaluate the effects of chitosan nanoparticles on cervical cancer cell proliferation. MTT (3-(4,5-dimethylthiazol-2-yl)-2,5-diphenyltetrazolium bromide) is a yellow tetrazolium salt absorbed by metabolically active cells, converting into purple formazan crystals through dehydrogenase enzyme activity.

In this experiment, 10,000 cells were placed in a 96 -well plate with complete culture medium to assess cell viability. PANC-1 cells were treated with aqueous sage extract and synthesized chitosan nanoparticles at various concentrations for 24 and 48 hours to determine IC50 values.

After incubation, 20 µL of MTT solution (0.5 mg/mL) was added to each well and incubated for 4 hours in the dark. The supernatant was discarded, and 150 µL of dimethyl sulfoxide (DMSO) was added to dissolve the formazan crystals. Absorbance was measured at 570 nm using an ELISA reader, allowing for the establishment of a standard curve correlating cell number with color intensity. This method quantifies cell viability and assesses the cytotoxic effects of chitosan nanoparticles on cancer cells.

2.9 Genes expression evaluation

RNA extraction is the first step in gene expression analysis. Following treatment of cancer and healthy cells with IC50 concentrations of synthesized chitosan nanoparticles in 6-well plates, RNA was extracted using the Trizol method. After washing the cells with PBS, Trizol was added to cover the wells, and the contents were transferred to microtubes. Chloroform was added, and the tubes were stored at -20°C for 24 hours before centrifugation, resulting in three phases. The upper aqueous phase containing RNA was transferred to new microtubes, mixed with cold isopropanol, and stored at -20°C for one hour. After a second centrifugation, 70% ethanol was added to the pellet, followed by another centrifugation. The supernatant was discarded, residual liquid was removed, and the tubes were inverted to evaporate ethanol. Finally, 25 µL of DEPC-treated water was added to the RNA pellet, which was stored at -70°C until use. To analyze the extracted RNA, the RNA samples were electrophoresed on a 1% agarose gel. Examination of the agarose gel using a gel doc system revealed three distinct bands of RNA.

After preparing equal concentrations of RNA, cDNA synthesis was performed using the RevertAid RT Reverse Transcription Kit from Thermo Fisher, following the provided protocol. Since DNA polymerase cannot use RNA as a template, an additional step was included in the PCR process. Here, RNA is converted to DNA using the enzyme reverse transcriptase for real-time PCR. In this experiment, cDNA was synthesized with the aid of random hexamers and stored at -70°C.

2.10 Primer Design

Primers are short strands of RNA or DNA, typically 18 to 22 bases long, that serve as starting points for DNA synthesis in PCR reactions. Proper primer design is crucial for the success of PCR. In this study, the Primer3 software was used to design primers, and the sequences of target genes were obtained from a genomic database (Table1).

2.11 Analysis of Gene Expression Changes in PI3K/AKT, EGFR, and P53 Using qRT-PCR

To detect and compare gene expression, qRT-PCR was performed using SYBR-Green PCR Master Mix and the Real-Time PCR Rotor-Gene 6000 device. The SYBR Green method is one of the most common approaches for conducting Real-Time PCR. This fluorescent dye emits fluorescence upon binding to double-stranded DNA in the minor groove. As the product amplification increases, more SYBR Green binds to the DNA, resulting in enhanced fluorescence intensity. The relative expression levels of the genes were assessed by comparing them to the control gene GAPDH, and the cycle thresholds (Ct) were calculated using the formula $2^{-\Delta\Delta Ct}2^{-\Delta\Delta Ct}$. Data analysis was conduct-

2.12 Statistical analysis

Statistical analysis was performed using SPSS 19 software (SPSS Inc., Chicago, IL, USA) and the results were analyzed by one-way ANOVA. The expression level of target genes between the treated samples and control group was measured by Tukey's HSD post hoc test. Data were presented as mean ± standard deviation (SD) and $p < .05$ was considered statistically significant.

3. Result

3.1 Scanning Electron Microscope analysis

The provided image is a Scanning Electron Microscope (SEM) micrograph of chitosan nanoparticles. The image clearly shows the structure and various sizes of the nanoparticles. The size range of the nanoparticles is from around 18.61 nm to 211.4 nm, indicating a broad size distribution of the synthesized chitosan nanoparticles.The nanoparticles appear as irregular agglomerates with porous and non-uniform surfaces. This morphology could be due to the aggregation of the nanoparticles or the specific characteristics of the material used in the synthesis process.

The scale bar at the bottom left of the image shows that each small division represents 100 nm, indicating that the image was captured at a magnification of 60,000x. These results can provide a better understanding of the physical and morphological properties of chitosan nanoparticles, which have various biomedical and drug delivery applications.

3.2 FTIR Analysis of Chitosan Nanoparticles and Drug-Loaded Nanoparticles

The FTIR spectrum of the chitosan nanoparticles showed a peak at 3419 cm^-1, which corresponds to the stretching vibrations of the NH2 and OH groups. The presence of peaks at 1655 and 1566 indicates the presence of the CONH2 and NH2 groups, respectively. Additionally, a peak at 1407 confirmed the presence of the CH2 group in the chitosan nanoparticles (Fig. 2). These results confirm the formation of the chitosan nanoparticles, corroborating the findings from previous studies. In the FTIR spectrum of the chitosan nanoparticles loaded with cisplatin and gemcitabine, the peak at 3510 indicates the presence of the NH and OH groups, suggesting the incorporation of gemcitabine and cisplatin. Furthermore, the peak at 2924 cm^-1 corresponds to the CH groups associated with the aliphatic structures of the nanocomplex. Additionally, the presence of the aromatic C=C groups of the nanocomplex was observed at the peak of 1361 (Fig. 3).

Table 1: Selected Genes primer specification

Primer Name		Sequence (5'to3')	Length	GC%	Tm° C
P53	Forward	CCTCAGCATCTTATCCGAGTGG	22	54.55	54.55
	Reverse	TGGATGGTGGTACAGTCAGAGC	22	54.55	54.55
EGFR	Forward	AACACCCTGGTCTGGAAGTACG	22	61.93	54.55
	Reverse	TCGTTGGACAGCCTTCAAGACC	22	62.75	54.55
Wee1	Forward	GATGTGCGACAGACTCCTCAAG	22	54.55	60.99
	Reverse	CTGGCTTCCATGTCTTCACCAC	22	54.55	61.45
AKT	Forward	TTCTGCAGCTATGCGCAATGTG	22	50	62.39
	Reverse	TGGCCAGCATACCATAGTGAGGTT	24	50	63.76
GAPDH	Forward	TGCCTCCTGCACCACCAAC	19	63.16	62.79
	Reverse	CGGAGGGGCCATCCACAG	18	72.22	62.18
PIK3CA	Forward	GGTTGTCTGTCAATCGGTGACTGT	24	50	63.03
	Reverse	GAACTGCAGTGCACCTTTCAAGC	23	52.17	63.17

These FTIR results provide evidence for the successful loading of the drugs, gemcitabine and cisplatin, into the chitosan nanoparticles, which is crucial for their potential biomedical and drug delivery applications.

3.3 Optimization of Chitosan Nanoparticle Concentration for MTT Assay

The MTT assay was used to measure the cytotoxic effects of the compounds of interest. The MTT assay was conducted to assess the cell toxicity of cisplatin, gemcitabine, and chitosan nanoparticles loaded with Gem+CP (gemcitabine + cisplatin) on HeLa cells after 24 and 48 hours of treatment.

The concentration of the drug that causes the death of 50% of the cells, or the IC50 value, was calculated for the 24-hour and 48-hour time periods using the Prism10 software.The IC50 value for cisplatin alone was found to be 21.97 µg/mL for the 24-hour treatment and 19.37 µg/mL for the 48-hour treatment (fig 4). The IC50 value for gemcitabine was found to be 13.76 µg/mL for the 24-hour treatment and 9.33 µg/mL for the 48-hour treatment (fig 5).

The treatment with CSNps-CP-Gem (chitosan nanoparticles loaded with gemcitabine and cisplatin) led to a significantly higher inhibition of cell viability compared to cisplatin and gemcitabine alone. The IC50 value for CSNps-CP-Gem was calculated to be 6.005 µg/mL at 24 hours and 4.050 µg/mL at 48 hours, The combination of CSNps-CP-Gem exhibited the strongest anti-tumor effect, with

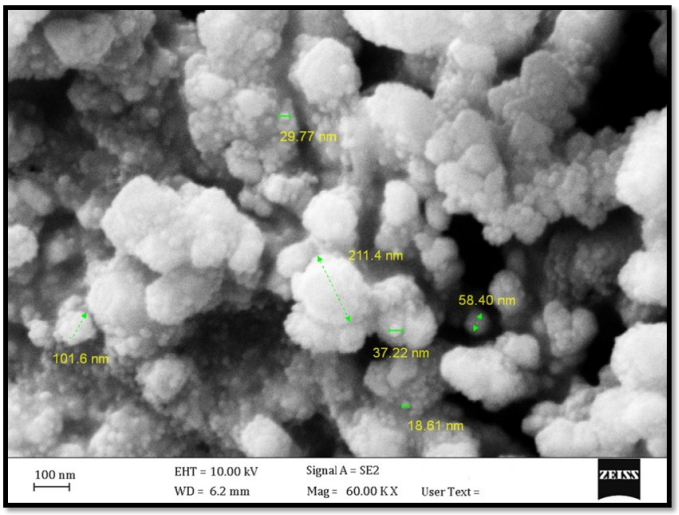

Figure 1. SEM micrograph of chitosan nanoparticles

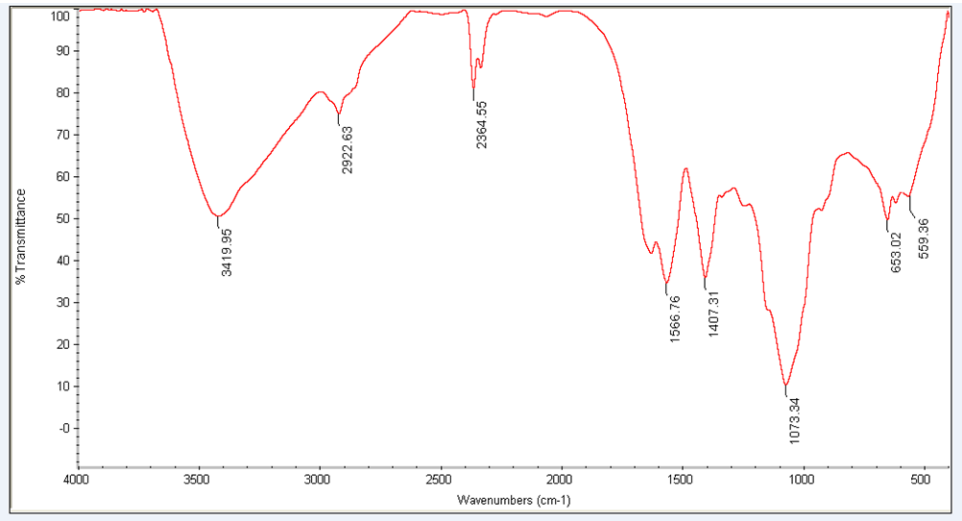

Figure 2. The FTIR spectrum of the chitosan nanoparticles

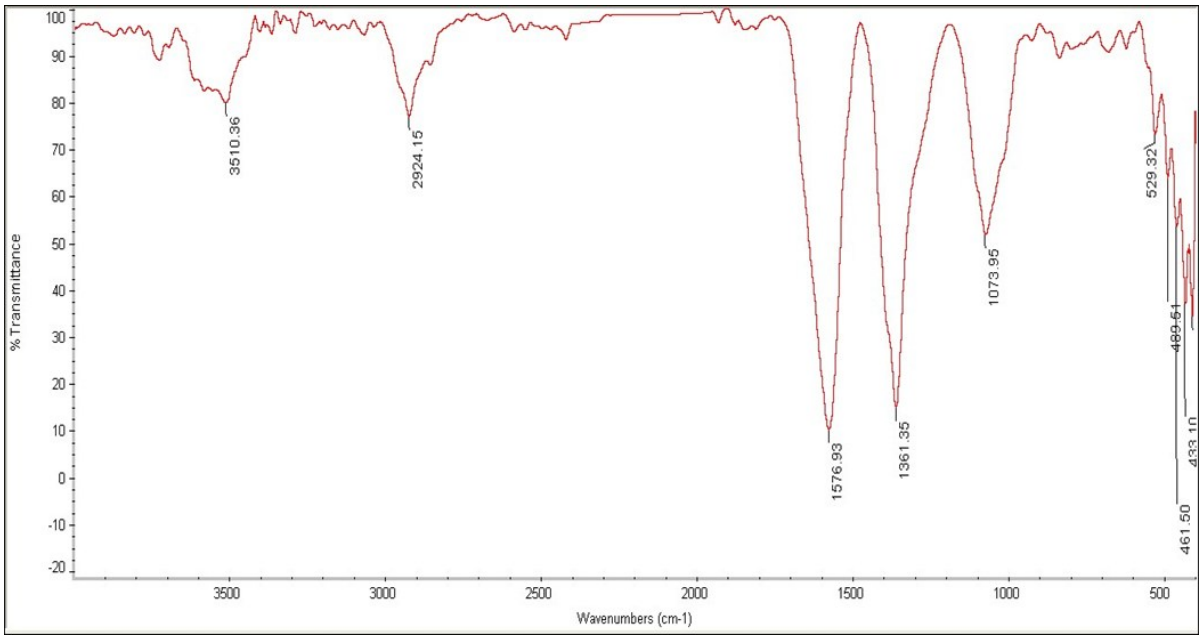

Figure 3. The FTIR spectrum of the CSNps-CP-Gem nanoparticles

an IC50 value of 6.005 µg/mL. One-way ANOVA analysis showed a statistically significant difference in the IC50 values between the different treatment groups ($p<0.0001$)(fig 6).

Cytotoxicity of CSNps-CP-Gem on Normal MRC-5 Cells, The cytotoxicity of CSNps-CP-Gem (chitosan nanoparticles loaded with gemcitabine and cisplatin) was also evaluated on normal MRC-5 cells.

The IC50 value for CSNps-CP-Gem on MRC-5 cells was found to be Greater than 100 µg/mL for the 24-hour treatment and Greater than 100 µg/mL for the 48-hour treatment (9).

3.4 Morphological Evaluation of HeLa Cells after Treatment with CSNps-CP-Gem

Observation of the control cells under an optical microscope showed that the cells had a normal shape and size. In the cells treated with different concentrations of CSNps-CP-Gem nanoparticles, morphological changes were observed. As the concentration of the nanoparticles increased, changes such as cell shrinkage and cytoplasmic detachment were observed. At higher nanoparticle concentrations, further changes like the extrusion of cellular contents and nuclear deformation were also seen (figure 8). Therefore, it can be concluded that the CSNps-CP-Gem nanoparticles induced morphological changes that led to cell death in the HeLa cells.

3.5 Gene Expression Analysis of PI3K/AKT, EGFR, and P53 Compared to Control Group

3.5.1 P13K gene expression analysis

The gene expression analysis revealed that the PI3K gene expression was significantly decreased in the treated cells compared to the control group. The efficiency of the reaction for both the target gene (PI3K) and the reference gene was 1.0, and the relative expression of the PI3K gene was 0.737, indicating a downregulation of this gene. The standard error for the PI3K expression was between 0.595 and 0.921, and the 95% confidence interval was in the range of 0.551 to 0.998.

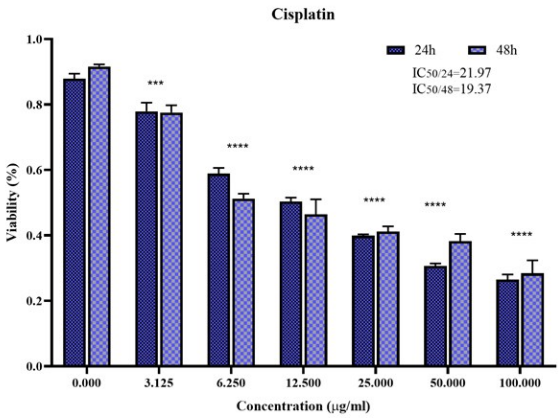

Figure 4. HeLa Cell Proliferation after Incubation with Cisplatin, Cisplatin has an anti-proliferative effect on HeLa cells at concentrations ranging from 3.125 to 100 µg/mL, at all time points (****p-value <0.0001).

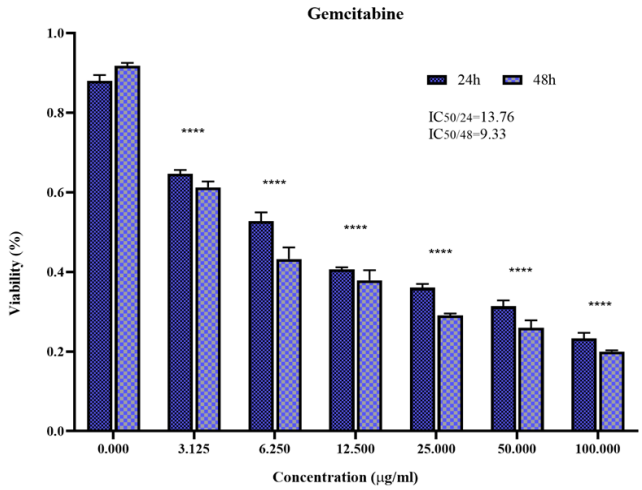

Figure 5. HeLa Cell Proliferation after Incubation with Gemcitabine, The results show that gemcitabine has an anti-proliferative effect on HeLa cells at concentrations ranging from 3.125 to 100 µg/mL, at all time points (****p-value <0.0001).

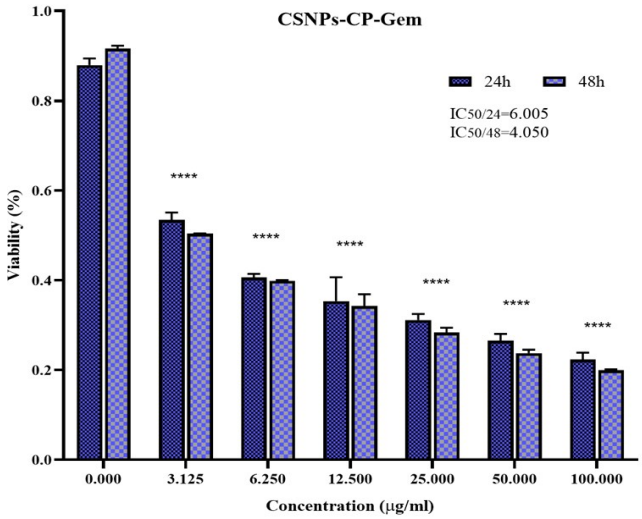

Figure 6. HeLa Cell Proliferation after Incubation with CSNps-CP-Gem, The results show that the CSNps-CP-Gem (chitosan nanoparticles loaded with gemcitabine and cisplatin) has an anti-proliferative effect on HeLa cells at concentrations ranging from 3.125 to 100 µg/mL, at all time points (****p-value <0.0001).

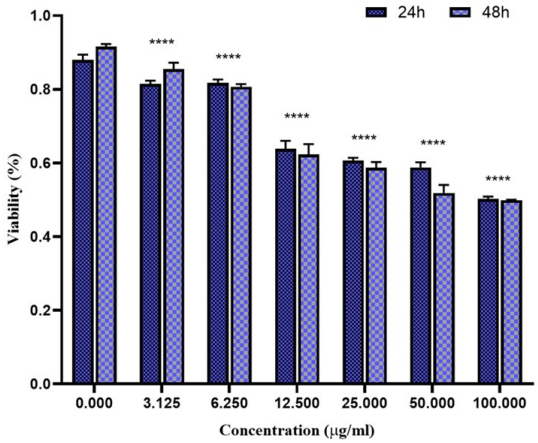

Figure 7. MRC-5 Cell Proliferation after Incubation with Different Concentrations of CSNps-CP-Gem for 24 and 48 Hours. CSNps-CP-Gem did not show any cytotoxicity at concentrations from 3.125 to 100 µg/mL (****p-value <0.0001).

The probability of the alternative hypothesis (P (H1)) was 0.000, which indicates the statistical significance of the results. These findings suggest that the PI3K/AKT signaling pathway may be downregulated in the HeLa cells treated with the CSNps-CP-Gem nanoparticles, which could be a potential mechanism underlying the cytotoxic effects observed in the previous experiments (Table 2) (Fig 9).

3.5.2 Gene Expression Analysis of AKT

The efficiency of the reaction for both the target gene (AKT) and the reference gene was 1.0. The relative expression of the AKT gene compared to the reference gene was measured at 0.664, indicating a significant decrease in its expression. The standard error for AKT expression ranged from 0.545 to 0.812, with a 95% confidence interval between 0.525 and 0.812. The probability of the alternative hypothesis (P(H1)) was 0.000, indicating the statistical significance of these results (Table 3).

Ultimately, the findings demonstrate that the expression of the AKT gene was significantly reduced, suggesting a potential downregulation of the AKT signaling pathway in response to the treatment (Fig 10).

3.5.3 Gene Expression Analysis of Wee1

The efficiency of the reaction for both the target gene (Wee1) and the reference gene was 1.0. The relative expression of the Wee1 gene compared to the reference gene was measured at 0.690, indicating a decrease in its expression. The standard error for Wee1 expression ranged from 0.574 to 0.830, with a 95% confidence interval between 0.568 and 0.839. However, the probability of the alternative hypothesis (P(H1)) was 0.339, indicating that this decrease in expression is not statistically significant (Table 4) . Consequently, the changes observed in the expression of the Wee1 gene do not demonstrate statistical significance (fig 11).

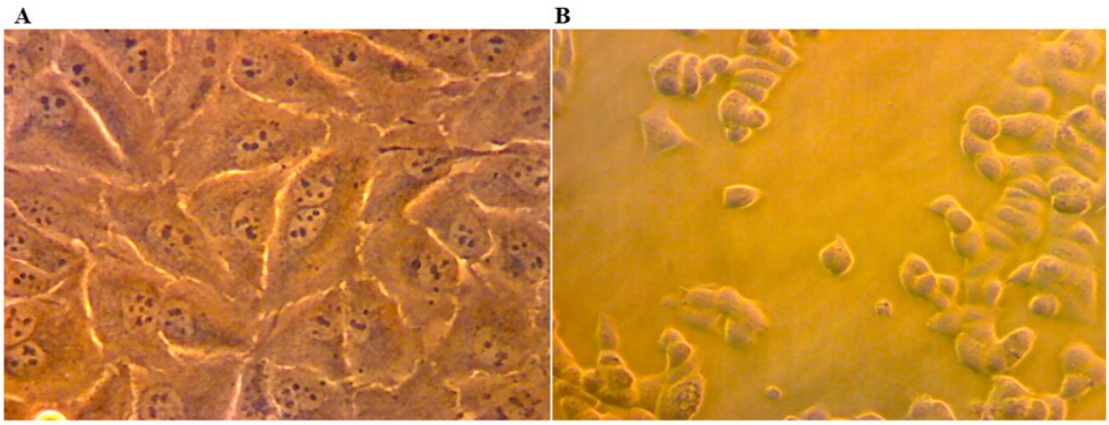

Figure 8. The images shows the morphological changes in HeLa cells after treatment with CSNps-CP-Gem (chitosan nanoparticles loaded with gemcitabine and cisplatin), A) Control HeLa cells: The cells exhibit a normal, healthy morphology with a well-defined shape and size. B) HeLa cells treated with CSNps-CP-Gem: The treated cells show various morphological changes, such as cell shrinkage, cytoplasmic detachment, and nuclear deformation, indicating the cytotoxic effects of the CSNps-CP-Gem nanoparticles.

Table 2: Relative Expression of PI3K Compared to Control

Gene	Type	Reaction Efficiency	Expression	Std. Error	95% C.I.	P(H1)	Result
GAPDH	REF	1.0	1.000				
PI3K	TRG	1.0	0.737	0.595 - 0.921	0.551 - 0.988	0.000	DOWN

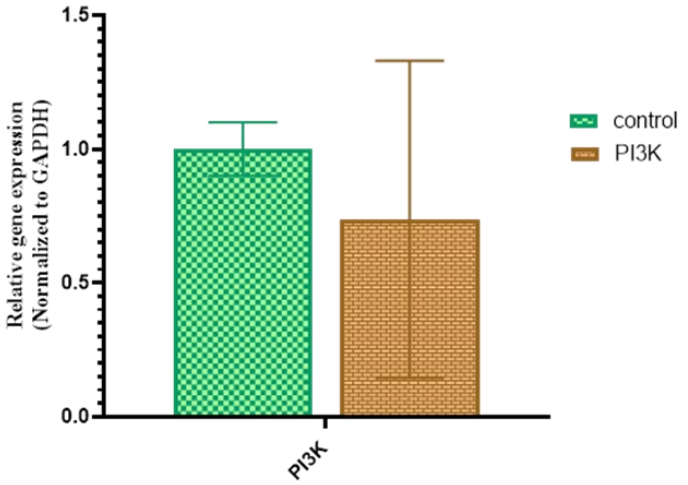

Figure 9. Comparative P13K gene expression

3.5.4 Gene Expression Analysis of P53

The efficiency of the reaction for both the target gene (P53) and the reference gene was 1.0. The relative expression of the P53 gene compared to the reference gene was measured at 2.274, indicating a significant increase in its expression. The standard error for P53 expression ranged from 2.040 to 2.537, with a 95% confidence interval between 1.983 and 2.608. The probability of the alternative hypothesis (P(H1)) was 0.000, indicating statistical significance of these results (Table 5). Ultimately, the findings demonstrate that the expression of the P53 gene has significantly increased, suggesting an active role of this gene in response to the treatment (Fig 12).

3.5.5 Gene Expression Analysis of EGFR

The relative expression of the EGFR gene The efficiency of the reaction for both the target gene

Table 3: Relative Expression of AKT Compared to Control

Gene	Type	Reaction Efficiency	Expression	Std. Error	95% C.I.	P(H1)	Result
GAPDH	REF	1.0	1.000				
AKT	TRG	1.0	0.664	0.545 - 0.812	0.525 - 0.841	0.000	DOWN

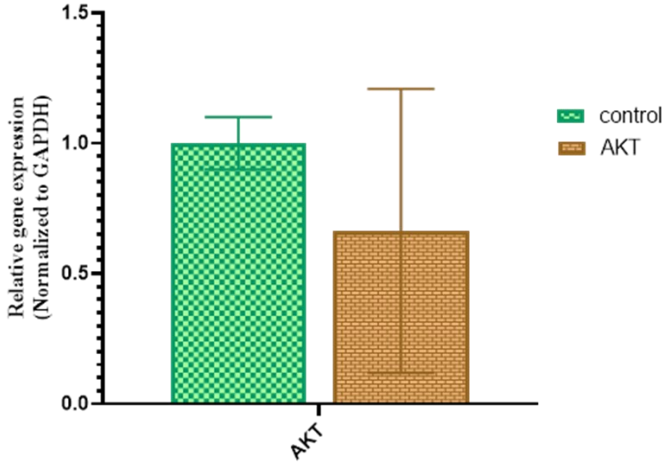

Figure 10. Comparative AKT gene expression

compared to the reference gene was measured at 0.578, indicating a significant decrease in its expression. The standard error for EGFR expression ranged from 0.506 to 0.671, with a 95% confidence interval between 0.457 and 0.735. The probability of the alternative hypothesis (P(H1)) was 0.000, indicating the statistical significance of these results (Table 6) . Ultimately, the findings demonstrate that the expression of the EGFR gene has significantly decreased, suggesting a potential downregulation of the EGFR signaling pathway in response to the treatment (Fig 13).

4. Discussion

Cervical cancer is the second most common cancer in the world. It is the fourth leading cause of cancer -related deaths among women globally, with over 85% of cases and deaths occurring in developing countries (2) Most cervical cancer cells are known to be infected with human papillomavirus (HPV), expressing the viral oncogenes E6 and E7, which suppress cellular regulatory proteins that play important roles in growth, differentiation, survival, apoptosis, and genome stability(23).

Table 4: Relative Expression of Wee1Compared to Control

Gene	Type	Reaction Efficiency	Expression	Std. Error	95% C.I.	P(H1) Result
GAPDH	REF	1.0	1.000			
Wee1	TRG	1.0	0.690	0.574 - 0.830	0.568 - 0.839	0.339

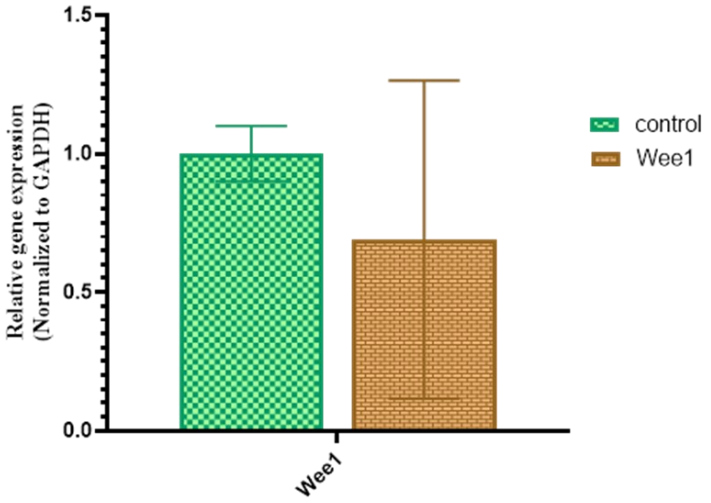

Figure 11. Comparative Wee1 gene expression

Table 5: Relative Expression of P53Compared to Control

Gene	Type	Reaction Efficiency	Expression	Std. Error	95% C.I.	P(H1) Result
GAPDH	REF	1.0	1.000			
P53	TRG	1.0	2.274	2.040 - 2.537	1.983 - 2.608	0.000 UP

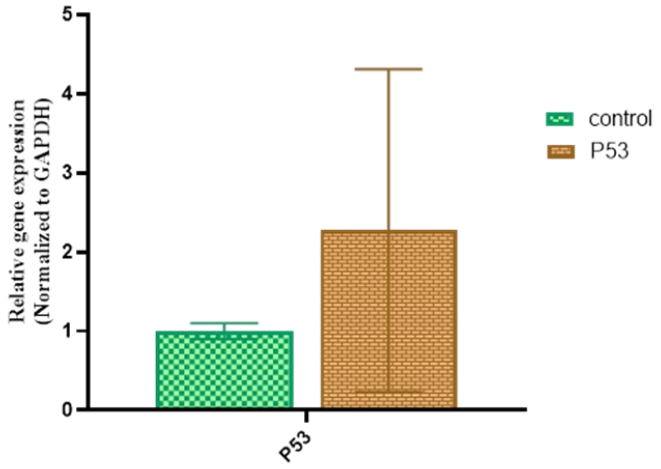

Figure 12. Comparative P53 gene expression

Table 6: Relative Expression of EGFR Compared to Control

Gene	Type	Reaction Efficiency	Expression	Std. Error	95% C.I.	P(H1)	Result
GAPDH	REF	1.0	1.000				
EGFR	TRG	1.0	0.578	0.506 - 0.671	0.457 - 0.735	0.000	DOWN

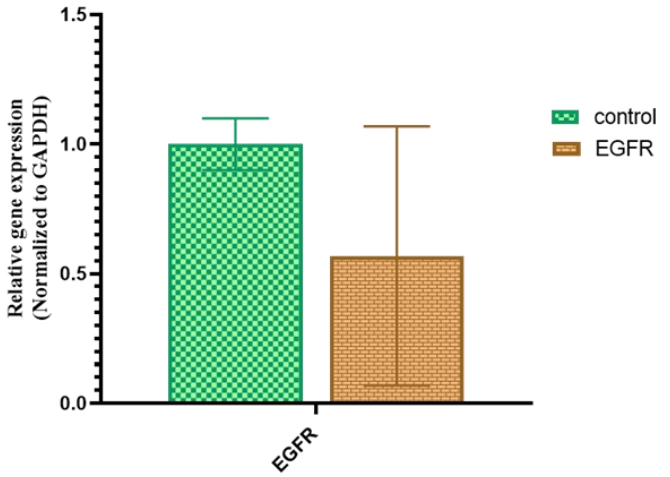

Figure 13. Comparative EGFR gene expression

The aim of this study is to investigate the effect of chitosan-cisplatin/gemcitabine nanoparticles on the PI3K/AKT, EGFR, P53, and Wee1 pathways in cervical cancer cells using real-time PCR. For this purpose, the HeLa cell line was first prepared. Then, chitosan nanoparticles were synthesized using chitosan and TPP, and finally conjugated with Gem/CS. Confirmation tests including SEM, FTIR, and UV-visible spectroscopy were performed to verify the synthesis of the nanoparticles. In the next step, the effect of CSNps-CP-Gem on HeLa cells was assessed using the MTT assay. Finally, the expression levels of the PI3K/AKT, EGFR, P53, and Wee1 genes were analyzed after treatment with the CSNps-CP-Gem nanoparticles using real-time PCR.

FTIR spectroscopy confirmed the encapsulation of CS/Gem in chitosan nanoparticles. Peaks corresponding to the functional groups of chitosan, the drug gemcitabine, and cisplatin were present in the FTIR spectrum. SEM images confirmed the spherical morphology and average size of less than 200 nanometers. These characterization tests validated the well-defined synthesis of chitosan nanoparticles that encapsulate Gm/CS with desirable properties. After treating HeLa cancer cells with various concentrations of CSNPs/Cp/Gem, including 0, 3.125, 6.25, 12.5, 25, 50, and 100 micrograms per milliliter for 24 and 48 hours, the cell viability was measured using the MTT method at a wavelength of 570 nanometers. The highest inhibition of cell proliferation was associated with the concentration of 100 micrograms/milliliter of CSNPs/Cp/Gem, while the minimum inhibition was observed at 3.125 micrograms/milliliter. The IC50 values for CSNPs/Cp/Gem were 6.005 and 4.05 micrograms per milliliter at 24 and 48 hours, respectively.

CSNPs/Cp/Gem significantly increased cytotoxicity. CSNPs/Cp/Gem exhibited higher toxicity compared to gemcitabine and cisplatin, attributed to the more targeted delivery of gemcitabine and cisplatin by the nanocarrier. Additionally, after treating the cells with the nanoparticles, the expression of P53 increased by a factor of 2.274 compared to the control group. The expression levels of EGFR, PI3K, and AKT significantly decreased by factors of 0.578, 0.737, and 0.664, respectively. The expression of WEE1 decreased, but this decrease was not significant.

In a similar study, Duygu Aydemir and colleagues investigated the effects of chitosan nanoparticles (NPs) loaded with gemcitabine (GEM) on pancreatic cancer cells, particularly CFPAC-1 cells. They showed that gem-containing nanoparticles significantly enhanced the apoptotic and ferroptotic responses in CFPAC-1 cells compared to treatment with GEM alone. This suggests that nanoparticles may improve the efficacy of gemcitabine in inducing cancer cell death. Additionally, empty chitosan nanoparticles did not show toxicity on L929 cells, indicating that the nanoparticles themselves are biocompatible and safe for use. Protein levels of ERK12 showed a significant increase in cells treated with gem-loaded nanoparticles at specific concentrations (32.1 and 64.2 micrograms per milliliter), while lower and higher concentrations resulted in a decrease. This suggests that ERK12 may play a role in response to GEM-loaded NPs and warrants further investigation (24). These results highlight the potential of using gemcitabine-loaded chitosan nanoparticles as a promising strategy to improve treatment outcomes in pancreatic cancer patients.

In another study, hybrid nanoparticles were developed and evaluated for effective intrauterine delivery of the anti-cancer drug gemcitabine in a rat model of cancer. The selected GEM-HNPs underwent further investigations regarding physical

morphology, solid-state characteristics, drug release percentage, in vitro cytotoxicity on HeLa cells, and in vivo cellular uptake using confocal laser microscopy. The efficacy and safety of GEM-HNPs for intrauterine delivery were compared with intravenous gemcitabine administration. The selected nanoparticles exhibited suitable characteristics such as a particle size of 235.9 ± 11.24 nanometers, a polydispersity index of 0.290 ± 0.004, a zeta potential of 43.8 ± 0.495 millivolts, a high loading efficiency of 76.8 ± 1.3 percent, complete drug release within 24 hours, increased intracellular uptake, and drug penetration in host tissue. The IC50 of gemcitabine alone did not show a significant difference compared to GEM-HNPs ($p<0.05$). The interstitial anti-tumor study showed that intrauterine delivery of GEM-HNPs successfully reduced acid trichloroacetic acid-induced host cancer. Consequently, the present study is the first to demonstrate a successful hybrid nanoparticle for vaginal delivery of GEM in the treatment of cervical cancer (26).

In a similar study, K. Venkates Kumar and colleagues synthesized chitosan nanoparticles containing sialic acid (SA) and cetuximab (Cxmab) loaded with gemcitabine (GMC). This study evaluated the preparation, physicochemical characteristics, in vivo effects, and interstitial targeting of chitosan nanoparticles containing sialic acid (SA) and cetuximab (Cxmab) loaded with gemcitabine (GMC) targeted to glycan receptors and EGFR in non-small cell lung cancer (NSCLC) A-549 cells. Results from cytotoxicity, bioavailability, and interstitial therapeutic effects indicated that the targeted formulations to EGFR and glycan (GMC-CSN-SA-Cxmab-NPs) had stronger anti-cancer activity compared to non-targeted formulations and specifically targeted NSCLC A-549 cells. Therefore, they could potentially serve as a suitable alternative to traditional chemotherapy (27).

In another study similar to ours, the effects of newly developed chitosan nanoparticles containing gemcitabine (Gem) along with cisplatin (DDP) on epithelial-mesenchymal transition (EMT), invasion, and cellular dissemination in pancreatic cancer were evaluated. 62 BALB/C mice were used for the subcutaneous tumor model. After determining the appropriate drug concentration, the animals were divided into control groups, chitosan glycol microcapsules (GC)-Gem, antibody complex (Abc)-GC-Gem, and Abc-GC-Gem microcapsules + DDP. Results showed that, compared to the control group, tumor size and weight decreased in the treatment groups, and apoptosis and drug toxicity increased. Additionally, the Abc-GC-Gem capsules + DDP group had a better effect than the other groups. Therefore, it can be concluded that gemcitabine nanoparticles in conjunction with cisplatin can inhibit the invasion and dissemination of pancreatic cancer cells and enhance the effect of chemotherapy (28).

In the study by Jing-yi Wang and colleagues, solid lipid nanoparticles (SLN) coated with chitosan and containing cisplatin (CDDP) were synthesized for the treatment of HeLa host cancer. The prepared nanoparticles were nanosized and demonstrated controlled drug release under physiological conditions. The empty nanoparticles exhibited high biocompatibility, indicating their suitability for cancer targeting. The substitution of CDDP in SLN resulted in increased mortality of cancer cells. Additionally, SLN coated with chitosan and containing CDDP (CChSLN) significantly reduced the survival ability of cancer cells even at lower concentrations. The higher toxicity of CChSLN was attributed to greater cellular uptake and

time-controlled drug release compared to CSLN. Researchers believe that this new formulation may be a suitable option for host cancer treatment and encourages future research (29).

In another study, NPs based on two oceanic-origin polymers (fucoidan and chitosan) were prepared using a complex polyelectrolyte for the delivery of the model anti-tumor drug (gemcitabine [Gem]). The final formulation resulted in stable NPs with a size of approximately 115-140 nanometers and a polydispersity index of less than 0.2. Gem was loaded into NPs with a maximum encapsulation yield of 35-42 percent. Drug release studies showed that approximately 84 percent of Gem was released within 4 hours. Similar to our study, toxicity results indicated that NPs containing Gem had 25 percent greater toxicity compared to free Gem without increasing toxicity on vascular cells. Drug-containing NPs exhibited greater toxicity on breast cancer cells without increasing toxicity on normal tissues (30).

5. Conclusion

In conclusion, this study demonstrates the promising potential of chitosan-cisplatin nanoparticles enhanced with gemcitabine in targeting cervical cancer cells through the modulation of key signaling pathways, specifically PI3K/AKT, EGFR, P53, and Wee1. The significant downregulation of PI3K, AKT, and EGFR, alongside the notable upregulation of P53 expression, suggests a robust mechanism by which these nanoparticles enhance cytotoxic effects while minimizing damage to normal tissues. The MTT assay results indicate that the CSNps-CP-Gem formulation exhibits superior anti-tumor efficacy compared to conventional treatments, highlighting its potential as a targeted therapeutic strategy. These findings contribute valuable insights into the development of more effective and less toxic treatment modalities for cervical cancer, paving the way for future research into nanoparticle-based therapies in oncology.

6. References

1.Zhang S, Xu H, Zhang L, Qiao Y. Cervical cancer: Epidemiology, risk factors and screening. Chinese Journal of Cancer Research. 2020;32(6):720–8.

2.Scott-Williams J, Hosein A, Akpaka P, Adidam Venkata CR. Epidemiology of Cervical Cancer in the Caribbean. Cureus. 2023 Nov 3;

3.yadav G, Srinivasan G, jain A. Cervical cancer: Novel treatment strategies offer renewed optimism. Pathol Res Pract. 2024 Feb;254:155136.

4.yadav G, Srinivasan G, jain A. Cervical cancer: Novel treatment strategies offer renewed optimism. Pathol Res Pract. 2024 Feb;254:155136.

5.Okunade KS. Human papillomavirus and cervical cancer. J Obstet Gynaecol. 2020 Jul;40(5):602–8.

6.Dillner J. Early detection and prevention. Mol Oncol. 2019 Mar 27;13(3):591–8.

7.Mir BA, Ahmad A, Farooq N, Priya MV, Siddiqui AH, Asif M, et al. Increased expression of HPV-E7 oncoprotein correlates with a reduced level of pRb proteins via high viral load in cervical cancer. Sci Rep. 2023 Sep 12;13(1):15075.

8.Chan CK, Aimagambetova G, Ukybassova T, Kongrtay K, Azizan A. Human Papillomavirus Infection and Cervical Cancer: Epidemiology, Screening, and Vaccination—Review of Current Perspectives. J Oncol. 2019 Oct 10;2019:1–11.

9.Jean S, Kiger AA. Classes of phosphoinositide 3-kinases at a glance. J Cell Sci. 2014 Mar 1;127(5):923–8.

10.He Y, Sun MM, Zhang GG, Yang J, Chen KS, Xu WW, et al. Targeting PI3K/Akt signal transduction for cancer therapy. Signal Transduct Target Ther. 2021 Dec 16;6(1):425.

11.Orofiamma LA, Vural D, Antonescu CN. Control of cell metabolism by the epidermal growth factor receptor. Biochimica et Biophysica Acta (BBA) - Molecular Cell Research. 2022 Dec;1869(12):119359.

12. An Z, Aksoy O, Zheng T, Fan QW, Weiss WA. Epidermal growth factor receptor and EGFRvIII in glioblastoma: signaling pathways and targeted therapies. Oncogene. 2018 Mar;37(12):1561–75.

13.Zhang L, Reue K, Fong LG, Young SG, Tontonoz P. Feedback Regulation of Cholesterol Uptake by the LXR–IDOL–LDLR Axis. Arterioscler Thromb Vasc Biol. 2012 Nov;32(11):2541–6.

14.Esposito F, Giuffrida R, Raciti G, Puglisi C, Forte S. Wee1 Kinase: A Potential Target to Overcome Tumor Resistance to Therapy. Int J Mol Sci. 2021 Oct 1;22(19):10689.

15.Geenen JJJ, Schellens JHM. Molecular Pathways: Targeting the Protein Kinase Wee1 in Cancer. Clinical Cancer Research. 2017 Aug 15;23(16):4540–4.

16.S. Gesto D, M.F.S.A. Cerqueira N, A. Fernandes P, J. Ramos M. Gemcitabine: A Critical Nucleoside for Cancer Therapy. Curr Med Chem. 2012 Mar 1;19(7):1076–87.

17.Anand U, Dey A, Chandel AKS, Sanyal R, Mishra A, Pandey DK, et al. Cancer chemotherapy and beyond: Current status, drug candidates, associated risks and progress in targeted therapeutics. Genes Dis. 2023 Jul;10(4):1367–401.

18.Samanta K, Setua S, Kumari S, Jaggi M, Yallapu MM, Chauhan SC. Gemcitabine Combination Nano Therapies for Pancreatic Cancer. Pharmaceutics. 2019 Nov 4;11(11).

19.Dasari S, Tchounwou PB. Cisplatin in cancer therapy: molecular mechanisms of action. Eur J Pharmacol. 2014 Oct 5;740:364–78.

20.Li Q, Chen S, Wang X, Cai J, Huang H, Tang S, et al. Cisplatin-Based Combination Therapy for Enhanced Cancer Treatment. Curr Drug Targets. 2024 May;25(7):473–91.

21.Gavas S, Quazi S, Karpiński TM. Nanoparticles for Cancer Therapy: Current Progress and Challenges. Nanoscale Res Lett. 2021 Dec 5;16(1):173.

22.Brianna, Lee SH. Chemotherapy: how to reduce its adverse effects while maintaining the potency? Medical Oncology. 2023 Feb 3;40(3):88.

23.Pal A, Kundu R. Human Papillomavirus E6 and E7: The Cervical Cancer Hallmarks and Targets for Therapy. Front Microbiol. 2020 Jan 21;10.

24.Aydemir D, Öztürk K, Arslan FB, Çalis S, Ulusu NN. Gemcitabine-loaded chitosan nanoparticles enhanced apoptotic and ferroptotic response of gemcitabine treatment alone in the pancreatic cancer cells in vitro. Naunyn Schmiedebergs Arch Pharmacol. 2024 Nov 17;397(11):9051–66.

25.Ferreira Soares DC, Domingues SC, Viana DB, Tebaldi ML. Polymer-hybrid nanoparticles: Current advances in biomedical applications. Biomedicine & Pharmacotherapy. 2020 Nov;131:110695.

26.Narváez-Narváez DA, Duarte-Ruiz M, Jiménez-Lozano S, Moreno-Castro C, Vargas R, Nardi-Ricart A, et al. Comparative Analysis of the Physicochemical and Biological Characteristics of Freeze-Dried PEGylated Cationic Solid Lipid Nanoparticles. Pharmaceuticals. 2023 Nov 9;16 (11):1583.

27.Kumar K, Rawat SG, Manjit, Mishra M, Priya, Kumar A, et al. Dual targeting pH responsive chitosan nanoparticles for enhanced active cellular internalization of gemcitabine in non -small cell lung cancer. Int J Biol Macromol. 2023 Sep;249:126057.

28.Yu H, Song H, Xiao J, Chen H, Jin X, Lin X, et al. The effects of novel chitosan-targeted gemcitabine nanomedicine mediating cisplatin on epithelial mesenchymal transition, invasion and metastasis of pancreatic cancer cells. Biomedicine & Pharmacotherapy. 2017 Dec;96:650–8.

29. Wang J yi, Wang Y, Meng X. Chitosan Nanolayered Cisplatin-Loaded Lipid Nanoparticles for Enhanced Anticancer Efficacy in Cervical Cancer. Nanoscale Res Lett. 2016 Dec 25;11(1):524.

30. 30.Oliveira C, Neves NM, Reis RL, Martins A, Silva TH. Gemcitabine Delivered by Fucoidan/Chitosan Nanoparticles Presents Increased Toxicity Over Human Breast Cancer Cells. Nanomedicine. 2018 Aug 7;13(16):2037–50.